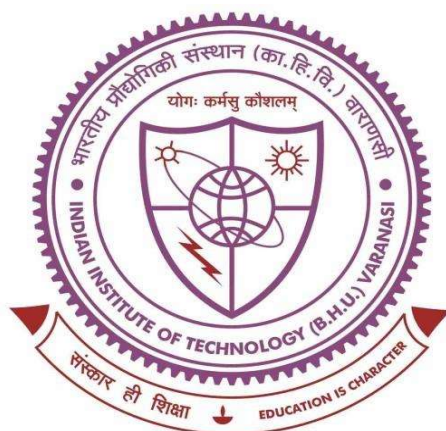


**SYNTHESIS AND PHYSICAL  
PROPERTIES OF ALKALINE EARTH  
METAL DOPED  $La_{9.67}Si_6O_{26.5}$   
OXYAPATITE SOLID ELECTROLYTE**



**THESIS SUBMITTED FOR THE AWARD OF THE DEGREE OF**

**Doctor of Philosophy**

**In**

**Physics**

**By**

**Ashishkumar Yadav**

**Under the supervision of**

**Prof. Prabhakar Singh**

DEPARTMENT OF PHYSICS  
INDIAN INSTITUTE OF TECHNOLOGY  
BANARAS HINDU UNIVERSITY  
VARANASI-221005  
INDIA

**Dr. Neetu Jha**

DEPARTMENT OF PHYSICS  
INSTITUTE OF CHEMICAL TECHNOLOGY  
ICT(MATUNGA), MUMBAI-400019  
INDIA

**15171001**

**2023**



*Dedicated*

*To*

*My son*



## CERTIFICATE

It is certified that the work contained in the thesis titled “SYNTHESIS AND PHYSICAL PROPERTIES OF ALKALINE EARTH METAL DOPED  $La_{9.67}Si_6O_{26.5}$  OXYAPATITE SOLID ELECTROLYTE” by “ASHISHKUMAR YADAV” (Roll No. 15171001), in partial fulfillment of the requirement for award of degree of **Doctor of Philosophy** at **Indian Institute of Technology (B.H.U), Varanasi** is a record of her own work carried out under my supervision and guidance and this work has not been submitted elsewhere for a degree.

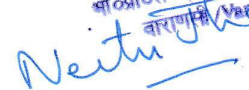
It is further certified that the student has fulfilled all the requirements of Comprehensive Examination, Candidacy, and SOTA for the award of Ph.D. Degree.

Date: 13/03/2023

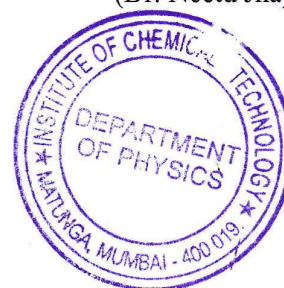
Place: Varanasi



**Supervisor**  
Dr. Prabhakar Singh  
(Prof. Prabhakar Singh)  
Professor  
भौतिकी विभाग / Dept. of Physics  
आर्य समाज (कोहि वि०) / IIT (BHU)  
वाराणसी / Varanasi-221005



**Co-Supervisor**  
(Dr. Neetu Jha)





### DECLARATION BY THE CANDIDATE

I, **ASHISHKUMAR YADAV** (Roll No. 15171001), certify that the work embodied in this thesis is my own bonafide work and carried out by me under the supervision of **PROF. PRABHAKAR SINGH and DR. NEETU JHA** from **JULY, 2015** to **DECEMBER 2022** at the **DEPARTMENT OF PHYSICS**, Indian Institute of Technology, Varanasi and Institute of Chemical Technology, Mumbai. The matter embodied in this thesis has not been submitted for the award of any other degree/diploma. I declare that I have faithfully acknowledged and given credits to the research workers wherever their works have been cited in my work in this thesis. I further declare that I have not willfully copied from any other's work, paragraphs, text, data, results, *etc.*, reported in journals, books, magazines, reports dissertations, theses, *etc.*, or available at websites and have not included them in this thesis and have not cited as my own work.

Date: 13/03/2023

Place: Varanasi




Signature of the Student

(ASHISHKUMAR YADAV)

### CERTIFICATE BY THE SUPERVISOR

It is certified that the above statement made by the student is correct to the best of our knowledge.



Supervisor

(Prof. Prabhakar Singh)

Dr. Prabhakar Singh

प्रचार्य/Professor

भौतिकी विभाग/Deptt. of Physics

भा.प्रौ.सं. (का.हि.वि.)/IIT (BHU)

वाराणसी/Varanasi-221005



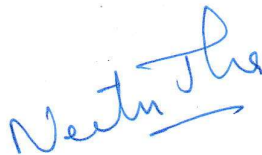
Signature of Head of Department

HEAD/विभागाध्यक्ष

भौतिकी विभाग/Deptt. of Physics

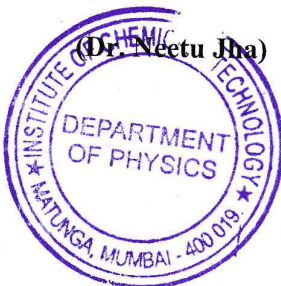
भा.प्रौ.सं./का.हि.वि./IIT (BHU)

वाराणसी/Varanasi-221005



Co-Supervisor

(Dr. Neetu Jha)





**COPYRIGHT TRANSFER CERTIFICATE**

**Title of the Thesis: "Synthesis and Physical Properties of Alkaline Doped  $La_{9.67}Si_6O_{26.5}$  Oxyapatite Solid State Electrolyte"**

**Name of the Student: Ashishkumar Yadav**

**Copyright Transfer**

**The undersigned hereby assigns to the Indian Institute of Technology (Banaras Hindu University) Varanasi all rights under copyright that may exist in and for the above thesis submitted for the award of the "*Doctor of Philosophy*".**

Date: 13/03/2023

Place: IIT (BHU), Varanasi



Signature of the Student

(ASHISHKUMAR YADAV)

**Note:** However, the author may reproduce or authorize others to reproduce material extracted verbatim from the thesis or derivative of the thesis for author's personal use provided that the source and the Institute's copyright notice are indicated.



---

---

## Acknowledgments

---

---

*“Hard work conquers all,” as the saying goes, but not entirely. This thesis is a reflection of my efforts. Still, it also includes contributions from many people who stood by my side during my time at the Indian Institute of Technology (Banaras Hindu University), Varanasi. It would give me great pleasure to acknowledge all those people in the following lines who stood by my side during the ups and down of my term as a Ph.D. scholar.*

*First and foremost, I would like to express my deep heart-felt gratitude to my thesis supervisor Prof. Prabhakar Singh, Department of Physics, Indian Institute of Technology (Banaras Hindu University) and Dr. Neetu Jha, Institute of Chemical Technology (Matunga) Mumbai, for advice, inspiration, and encouragement in pursuing my scientific interest. I will never forget your positive attitude towards nourishing my personality as well. It has been both a privilege and pleasure to have been associated with him.*

*I would also like to express my sincere thanks to RPEC member’s Prof. Sandip Chatterjee, Department of Physics, Indian Institute of Technology (Banaras Hindu University) and Prof. A. K. Singh, School of Materials Science & Technology, Indian Institute of Technology (Banaras Hindu University), for their valuable suggestions and critical remarks without which this work would not have been completed.*

*I also wish to express my sincere gratitude to all the teachers of the Department Prof. B.N. Dwivedi, Prof. D. Giri, Prof. R. Prasad, Dr. P. C. Pandey, Dr. Anita Mohan, Dr. Shail Upadhyay, Dr. S. K. Mishra, Dr. A. K. Srivastava, Dr. S. K. Singh, Dr. Avanish Singh Parmar, Dr. Saurabh Tripathi, Dr. Awaneesh Singh, Dr. R. K. Singh, Dr. Swapnil Patil, Dr. Shradha Mishra, Dr. Prasun Dutta, Dr. Rajeev Singh, Dr. Somnath Nag, Dr. Gauhar Abbas for their kind support at all moment during the progress of my research. I acknowledge the help and co-operation of all office staff of the Department and authorities of IIT (BHU) for their kind support during my stay to complete the thesis work.*

*I would like to thank Dr. Usha Mukundan, director and former Principal of Ramniranjan Jhunjhunwala College and Dr. Himanshu Dawda Principal of RJ college, for providing the all-possible co-operation and administrative help for my research work. I am also thankful to Dr. Neeta Srivastava, Dr. Devraj Pawar, Dr. Kiran Kolwankar , Dr. Vaishali Raikwar and Prof. Sandip Hinge), for providing the all departmental co-operation for completing my thesis work.*

*I would like to thank Dr. Pardeep K. Jha and Dr. Priyanka A. Jha, Department of Physics, IIT (BHU), Varanasi, Dr. Raghvendra Pandey and Dr. Onkarnath Verma for their invaluable suggestions scientific views in resolving lots of difficulties which I faced during my research work.*

*Mrs. Sandhya Yadav, my wife and my best friend, deserves a special thank you for her for sharing all my joys and sorrows over the previous several years. I greatly value your contribution and sincerely appreciate your belief in me. Thank you for always being there for me, especially when I needed you the most.*

*I sincerely acknowledge the help from my seniors Dr. Bheeshma Pratap Singh, Dr. Vani Pawar and Dr. Pravin Kumar. Special thanks to my friend and lab mate Dr. Ajay Bangwal, for his help and cooperation whenever needed. I also acknowledge my other lab mates Dr. Manish Kumar, Dr. Pragati Singh, Mr. Prem Chand Bharti, Ms. Uma Sharma, Mr. Ashish Kumar Ranjan, Ms. Kamana, Ms. Manisha Sharma, Ms. Swarnima Singh, Mr. Jay Narayan Mishra, Ms. Gargi and Mr. Hemant Yadav. Thank you all. You always made my life in the lab so pleasant.*

*Next, there are all the friends I've made on the campus, the list is too long to mention, but their friendship helped me make my stay in IIT(BHU) happy. I shall never forget the time with Dr. Pravin kumar, Dharmendra, Suraj, Vijay, Vinod, Chinmoy, Debojyoti, Pavan, Sadik, Ritika, Prajyoti, Ruchi, Yamini, Brijesh and many more.*

*The word 'thanks' look meaningless to express my gratitude to my friends Mr. Brijesh Yadav, Mr. Suraj Yadav, Mr. Yogesh Gupta, Mr. Jagdish Hande, Mr. Adwait Kulkarni, Rohit Chaudhary, Ms. Rani Shaikh, Ms. Kirti Singh, Mr. Jayshankar Singh, Mr. Rahul Tiwari, Mr. Bhagirat Mishra, Abhishek, Vikas*

and Akash. I want to express my gratitude to all of you for bringing pleasure, laughter, and celebration into my life.

I am forever indebted to my beloved father, Mr. Subhash Yadav, and my mother, Mrs. Champadevi Yadav, for their inseparable support and prayers. I feel a deep sense of gratitude for my parents, who formed a part of my vision and taught me the good things that matter in life. I am grateful to my brother Mr. Manish Yadav for their unending love and faith in me. A special thank you to my wife Mrs. Sandhya Yadav for making my life joyful and her unconditional support in my ups and down situations. I sincerely hope this thesis makes my family feel proud of me.

The financial help from the institute is duly acknowledged. With a deep sense of gratitude, I express my sincere thanks to CIFC, IIT (BHU), Varanasi for help in carrying out the characterization of the synthesized samples.

I also thank all those who could not find a separate mention but have helped me directly or indirectly in completing this gigantic task.

Finally, I bow before the almighty for being kind enough to provide me with the patience and knowledge to complete this research work. I dedicated this piece of work to the lord of the universe 'Mahadev' who was always there holding my hand throughout this journey of my Ph.D. and the journey of my life.

**Date:** 04/06/2023

**Place:** Varanasi



**(Ashishkumar Yadav)**



## Content

<b>CERTIFICATE.....</b>	<b>i</b>
<b>DECLARATION BY THE CANDIDATE .....</b>	<b>iii</b>
<b>COPYRIGHT TRANSFER CERTIFICATE .....</b>	<b>v</b>
<b>Acknowledgments .....</b>	<b>vii</b>
<b>Content .....</b>	<b>xi</b>
<b>LIST OF FIGURES.....</b>	<b>xv</b>
<b>LIST OF TABLES .....</b>	<b>xxiii</b>
<b>PREFACE .....</b>	<b>xxv</b>
<b>Chapter-1 .....</b>	<b>1</b>
<b>CHAPTER 1: Introduction and Literature Review .....</b>	<b>3</b>
<b>1.1 Motivation of the work.....</b>	<b>3</b>
<b>1.2 Fuel Cells.....</b>	<b>6</b>
<b>1.3 Types of Fuel Cell.....</b>	<b>7</b>
<b>1.4 Solid Oxide Fuel Cell (SOFC) .....</b>	<b>8</b>
1.4.1 General Introduction.....	8
1.4.2 Operation of Solid Oxide Fuel Cells.....	9
1.4.3 High and Intermediate Temperature Solid Oxide Fuel Cells .....	11
<b>1.5 Application Areas .....</b>	<b>13</b>
<b>1.6 Different Components of SOFCs .....</b>	<b>14</b>
1.6.1 Electrodes (Cathode and Anode) .....	14
1.6.2 Electrolyte.....	16
1.6.3 Interconnect .....	16
<b>1.7 Materials Selection for SOFCs .....</b>	<b>17</b>
1.7.1 Factors influencing ionic conduction of the electrolyte .....	18

<b>1.8 Present Scenario of electrolyte for Solid Oxide Fuel Cells .....</b>	<b>19</b>
<b>1.9 Apatite-type Materials .....</b>	<b>20</b>
1.9.1 Conductivity Optimization.....	23
1.9.2 Conduction mechanism in Apatite germinate: .....	26
1.9.3 AO <sub>6</sub> Metaprism Twist Angle in Apatite-type Materials .....	30
<b>1.10 Objective of Present Investigation.....</b>	<b>32</b>
<b>Chapter-2 .....</b>	<b>35</b>
<b>Chapter 2: Synthesis, Characterizations and Analysis Techniques .....</b>	<b>37</b>
<b>2.1 Overview .....</b>	<b>37</b>
2.1.1 Specification of Raw Materials .....	38
<b>2.2 Materials Synthesis.....</b>	<b>39</b>
2.2.1 SSR (Solid-State Reaction Route) .....	40
2.2.2 Mechanism of Ball-Mill.....	41
2.2.3 Preparation of Materials using Ball Milling.....	43
2.2.4 Calcination of Materials .....	44
2.2.5 Granulation and pelletization .....	44
<b>2.3 Pelletization for Conductivity and Dilatometry Measurements.....</b>	<b>45</b>
2.3.1 Sintering.....	46
<b>2.4 Characterization Techniques .....</b>	<b>46</b>
2.4.1 TGA-DSC (Thermal Analysis).....	46
2.4.2 Measurement of Density and Porosity .....	48
2.4.3 X-Ray Diffraction Analysis (XRD) .....	49
2.4.4 XPS (X-Ray Photoelectron Spectroscopy) .....	63
2.4.5 Scanning Electron Microscopy (SEM) .....	65
2.4.6 Ultra – Violet Visible (UV-Vis) Spectroscopy .....	67
2.4.7 Photoluminescence Spectroscopy (PL).....	69

2.4.8	Fourier Transform Infrared Spectroscopy (FTIR) .....	71
<b>2.5</b>	<b>Electrical Data Analysis .....</b>	<b>72</b>
2.5.1	Impedance Spectroscopy Analysis .....	74
2.5.2	Conductivity Spectroscopy Technique .....	79
<b>2.6</b>	<b>Analysis Techniques .....</b>	<b>81</b>
2.6.1	Process of Analysing the Obtained Data .....	81
<b>2.7</b>	<b>Theoretical Studies .....</b>	<b>82</b>
2.7.1	Bond Valance Energy-Based Approach .....	82
<b>Chapter-3</b>	<b>.....</b>	<b>85</b>
<b>CHAPTER 3: Ion transport and one-dimensional ion migration in lanthanum silicate apatite (La<sub>9.67</sub>Si<sub>6</sub>O<sub>26.5</sub>) .....</b>		<b>87</b>
<b>3.1</b>	<b>Introduction .....</b>	<b>87</b>
<b>3.2</b>	<b>Materials and Methods .....</b>	<b>89</b>
<b>3.3</b>	<b>Results and discussion: .....</b>	<b>90</b>
<b>3.4</b>	<b>Conclusions: .....</b>	<b>101</b>
<b>Chapter-4</b>	<b>.....</b>	<b>103</b>
<b>CHAPTER 4: Influence of ionic radii on the conduction mechanism in Lanthanum silicate oxyapatite.....</b>		<b>105</b>
<b>4.1</b>	<b>Introduction .....</b>	<b>105</b>
<b>4.2</b>	<b>Composition section .....</b>	<b>107</b>
<b>4.3</b>	<b>MATERIALS AND METHODS .....</b>	<b>109</b>
4.3.1	Sample preparations.....	109
4.3.2	Characterization techniques.....	110
<b>4.4</b>	<b>Results and Analysis .....</b>	<b>111</b>
4.4.1	Structural Studies .....	111
4.4.2	SEM Analysis: .....	119
4.4.3	XPS and TGA Studies.....	121

4.4.4 Temperature dependence conduction behaviour .....	128
<b>4.5 DISCUSSION AND CONCLUDING REMARK.....</b>	<b>143</b>
<b>Chapter-5 .....</b>	<b>147</b>
<b>CHAPTER 5: Overlapping large polaron tunnelling in lanthanum silicate oxyapatite ..</b>	<b>149</b>
<b>5.1 INTRODUCTION .....</b>	<b>149</b>
<b>5.2 Materials and Methods .....</b>	<b>151</b>
5.2.1 Sample preparation.....	151
<b>5.3 Characterization techniques .....</b>	<b>152</b>
<b>5.4 RESULTS AND ANALYSIS.....</b>	<b>153</b>
5.4.1 Structural Studies .....	154
<b>5.5 Temperature dependence conduction behaviour .....</b>	<b>163</b>
5.5.1 dc Conductivity .....	163
5.5.2 The universal exponent 'p' .....	164
<b>5.6 Frequency dependent conductivity behaviour .....</b>	<b>165</b>
5.6.1 The exponent parameter (s).....	165
<b>5.7 Optical absorption.....</b>	<b>168</b>
<b>5.8 DISCUSSION .....</b>	<b>171</b>
<b>5.9 CONCLUDING REMARKS .....</b>	<b>175</b>
<b>Chapter-6 .....</b>	<b>177</b>
<b>CHAPTER 6: Conclusions and Future Scopes .....</b>	<b>179</b>
<b>6.1 Conclusion of the Present Investigation.....</b>	<b>179</b>
<b>6.2 Scope for Future Work (New Directions and Future Perspectives) .....</b>	<b>181</b>
<b>References .....</b>	<b>185</b>
<b>Publications.....</b>	<b>215</b>

---

## LIST OF FIGURES

---

		Page No.
<b>Chapter 1</b>	<b>Introduction and Literature Review</b>	
Fig. 1.1	Energy demand and its consumption	4
Fig.1.2	Operation principle of a SOFC	9
Fig.1.3	Tubular SOFC configuration	10
Fig.1.4	Configuration for a planar design SOFC	11
Fig.1.5	Application of SOFC	14
Fig.1.6	(a) The major sources of ionic carriers in oxides and their respective mobilities compiled from literatures (b) The correlation of composition, microstructure, processing and electrical conductivity in polycrystalline materials under given temperature and surrounding atmosphere	19
Fig.1.7	Present Scenario of electrolytes	20
Fig.1.8	Conductivity of oxygen ion conductor including candidate SOFC electrolytes	21
Fig1.9	Apatite structure display	23
Fig1.10	Bulk conductivity maps	24
Fig1.11	A study of the conductivity of oxygen stoichiometric samples with the equal amount of A cation shows that doping the samples with lower valent dopants has a favorable effect on the La site but a deleterious effect on the Si site	25
Fig1.12	(a) The atomistic simulation investigations revealed an interstitial oxide-ion migration pathway through the channel in $\text{La}_{9.67}\text{Si}_6\text{O}_{26.5}$ , as well as a probable mechanism for such a sinusoidal pattern. (b) View from a wider angle that shows how Si polyhedra relax and turn	27
Fig1.13	(a) Diagrammatic sequence depicting the production and migration of the $(2\text{O}_i'' + \text{V}_\text{o}^{\bullet\bullet})$ defect complex, which is accomplished by a “push-pull” process down the c-axis and in the direction of the electron cloud. (b) Nonlinear $\text{O}_i''$ migration on the ab plane as a result (top view).	29
Fig1.14	The $\text{LaO}_6$ metaprism twist angle is $22.24^\circ$ in this polyhedral model of $\text{La}_{9.67}\text{Si}_6\text{O}_{26.5}$	30
Fig1.15	Examples of apatites have different metaprism twist angle $\phi$	31
Fig1.16	Comparison of conductivity data for selected oxide-ion conductors	33

<b>Chapter 2</b>	<b>Synthesis, Characterization and Analysis Techniques</b>	
Fig. 2.1	Schematic of Solid state reaction route	41
Fig. 2.2	Working Principle of Lab Ball-Miller	43
Fig. 2.3	Experimental setup of hydraulic press machine	45
Fig. 2.4	(a) TGA-DSC facility (b) experimental setup of TGA/DSC (right).	47
Fig. 2.5	Density kit and weighing balance	49
Fig. 2.6	(a) Visualization of Bragg's law (b) Schematic representation of $\theta/2\theta$ diffraction in Bragg-Brentano geometry	51
Fig. 2.7	Experimental setup of X-ray diffractometer	52
Fig. 2.8	XRD facilities, Central Instrument Facility	54
Fig. 2.9	A typical FullProf software interface during Rietveld refinement process	57
Fig. 2.10	(a) Mechanism and (b) Experimental setup for the XPS spectroscopy	65
Fig. 2.11	(a) Mechanism and (b) Experimental setup of SEM measurement	66
Fig. 2.12	Experimental setup of UV-Visible measurement	69
Fig. 2.13	Mechanism and experimental setup of photoluminescence spectroscopy	70
Fig. 2.14	(a) Mechanism and (b) experimental setup of Fourier transform infrared spectroscopy	71
Fig. 2.15	Experimental set up of automated impedance analyzer along with sample holder and furnace	73
Fig. 2.16	The equivalent circuit corresponds to the polycrystalline sample and their frequency response in the complex impedance plot.	79
Fig. 2.17	A typical conductivity spectrum of a polycrystalline material	81
<b>Chapter 3</b>	<b>Ion transport and one-dimensional ion migration in lanthanum silicate apatite (<math>La_{9.67}Si_6O_{26.5}</math>)</b>	
Fig.3.1	X-ray diffraction pattern of calcined powder of lanthanum silicate apatite (LSO)	91
Fig.3.2	Rietveld refinement pattern of calcined lanthanum silicate apatite ( $La_{9.67}Si_6O_{26.5}$ ; LSO) powder	92
Fig.3.3	Simultaneous DSC and TGA curve of calcined lanthanum silicate apatite ( $La_{9.67}Si_6O_{26.5-\delta}$ ) powder	94
Fig.3.4	(a) SEM microstructure of lanthanum silicate apatite (LSO) at 2 $\mu$ m, (b) at 10 $\mu$ m and (c) EDX analysis of the sample (d) grain size distribution (e) EDS distribution of the elements	95

Fig.3.5	Conductivity spectra of lanthanum silicate apatite (LSO) at 400-700 °C	97
Fig.3.6	Arrhenius representation of dc conductivity for lanthanum silicate apatite (LSO)	98
Fig. 3.7	Changes in the power exponent ‘n’ with temperature	99
Fig. 3.8	(a) Crystal structure of LSO (a-b axis view) with ion-migration iso-surface. (b) Oxygen ion diffusion migration barrier landscape for LSO derived from the bond valence energy model.	100
<b>Chapter 4</b>	<b>Influence of ionic radii on the conduction mechanism in Lanthanum silicate oxyapatite</b>	
Fig.4.1	Variation of La content with O vacancies on varying x	107
Fig.4.2	Variation of ion mobility volume with average ionic radii at La site	109
Fig.4.3	(a) Rietveld refinement of X-ray diffractograms of Ba substituted samples with P6 <sub>3</sub> /m symmetry using Full Prof Suite package with Pseudo-Voigt peak profile. The goodness of fit ( $\chi^2$ ) is lying within the appreciable range (Fig.4.2(a)). (b) splitting of the peak corresponding to $2\theta \approx 32^\circ$ reducing with the increase in x.	112
Fig.4.4	(a) Rietveld refinement of X-ray diffractograms of Ca substituted samples with P6 <sub>3</sub> /m symmetry using Full Prof Suite package with Pseudo-Voigt peak profile. The goodness of fit ( $\chi^2$ ) is lying within the appreciable range (Fig.4.3(a)). (b) splitting of the peak corresponding to $2\theta \approx 32^\circ$ disappearing with the increase in x	113
Fig.4.5	(a-b) Variation of Lattice parameters, La1(6h)-O4 bond distance of Ba modified $(La_{1-x}Ba_x)_{9.67}(SiO_4)_6O_{2+\delta}$ (x = 0.0, 0.05, 0.10 and 0.15)	115
Fig.4.6	(a-b) Variation of Lattice parameters, La1(6h)-O4 bond distance of Ca modified $(La_{1-x}Ca_x)_{9.67}(SiO_4)_6O_{2+\delta}$ (x = 0.0, 0.05, 0.10 and 0.15)	116
Fig.4.7	SEM micrographs and grain histograms of Ba modified $(La_{1-x}Ba_x)_{9.67}(SiO_4)_6O_{2+\delta}$ (x = 0.0, 0.05, 0.10 and 0.15)	119
Fig.4.8	SEM micrographs and grain histograms of Ca modified	120

	$(La_{1-x}Ca_x)_{9.67}(SiO_4)_6O_{2+\delta}$ ( $x = 0.0, 0.05, 0.10$ and $0.15$ )	
Fig. 4.9	Thermogravimetric curves for Ba modified $(La_{1-x}Ba_x)_{9.67}(SiO_4)_6O_{2+\delta}$ ( $x = 0.0, 0.05, 0.10$ and $0.15$ ) showing the variation of mass loss and $dm/dT$ with temperature	122
Fig.4.10	Thermogravimetric curves for Ca modified $(La_{1-x}Ca_x)_{9.67}(SiO_4)_6O_{2+\delta}$ ( $x = 0.0, 0.05, 0.10$ and $0.15$ ) showing the variation of mass loss and $dm/dT$ with temperature	123
Fig.4.11	Deconvoluted X-ray photoelectron spectroscopy measurements of Ba modified $(La_{1-x}Ba_x)_{9.67}(SiO_4)_6O_{2+\delta}$ ( $x = 0.0, 0.05, 0.10$ and $0.15$ )	124
Fig.4.12	Deconvoluted X-ray photoelectron spectroscopy measurements of Ca modified $(La_{1-x}Ca_x)_{9.67}(SiO_4)_6O_{2+\delta}$ ( $x = 0.0, 0.05, 0.10$ and $0.15$ )	126
Fig.4.13	$\sigma_{dc}-T$ plot for Ba and Ca substituted samples with nearest neighbour hopping	129
Fig.4.14	Arrhenius plots for Ca and Ba substituted $(La_{1-x}A_x)_{10-\alpha}(SiO_4)_6O_{2+\delta}$ ( $x = 0.0, 0.05, 0.10$ and $0.15$ )	130
Fig.4.15	a) Activation energies for Ca and Ba substituted $(La_{1-x}A_x)_{10-\alpha}(SiO_4)_6O_{2+\delta}$ ( $x = 0.0, 0.05, 0.10$ and $0.15$ ) and b) shows the structure for the movement of interstitial oxygen vacancies, La1 and La2 form concentric hexagons in a-b plane with O4 in center and further O4 forms a channel along c-axis as shown in (c)	131
Fig. 4.16	Variation of conductivity at 973 K with ion mobility volume for Ca and Ba substituted samples (inset) Variation of conductivity at 973 K with x	132
Fig. 4.17	Comparative of Rietveld refinement of $x = 0.0$ and Ca and Ba substituted samples with $x = 0.1$	132
Fig. 4.18	Variation of grain size and morphology with x for parent and Ca and Ba substituted samples	134
Fig. 4.19	TGA for $x = 0.0$ , $x= 0.1$ Ba and $x= 0.1$ Ca substituted	134

	samples in $(La_{1-x}A_x)_{9.67-\alpha}(SiO_4)_6O_{2+\delta}$	
Fig. 4.20	Deconvoluted XPS spectra corresponding to La, Ba, Ca, Si and O for $x = 0.0$ , $x = 0.1$ Ba and $x = 0.1$ Ca substituted samples in $(La_{1-x}A_x)_{9.67-\alpha}(SiO_4)_6O_{2+\delta}$	136
Fig. 4.21	(a) Grain size obtained from SEM micrographs (grain histograms) for Ca and Ba substituted samples (b) La+ Ba content extracted from XPS, La+Ca content extracted from XPS (c) Si content from XPS (d) O content from XPS (lines are a glide to eye)	138
Fig. 4.22	Nyquist plots taken over a wide frequency range (20 Hz to 1 MHz) at different temperatures	139
Fig. 4.23	Arrhenius plots for the grain, grain-boundary and electrode resistances	141
Fig. 4.24	Value of mean free ion lifetime with $x$	142
Fig. 4.25	Variation of (a) percolation energy along the x-axis (PEX) and z-axis (PEZ), (b) lattice parameters $a$ and $c$ , (c) PEZ, activation energy ( $E_a$ ) and band gap energy ( $E_g$ ), and (d) grain size and conductivity with average ionic radii at La site $\langle R_i, La \rangle$ .	144
<b>Chapter 5</b>	<b>Overlapping large polaron tunnelling in lanthanum silicate oxyapatite</b>	
Fig.5.1	(a) Rietveld refinement of X-ray diffractograms with P63/m symmetry using Full Prof Suite package with Pseudo-Voigt peak profile. The goodness of fit ( $\chi^2$ ) is lying within the appreciable range (Fig.5.1(a)). (b) splitting of the peak corresponding to $2\theta \approx 32^\circ$ disappearing with the increase in $x$	154
Fig.5.2	(a-b) Variation of Lattice parameters, La1(6h)-O4 bond distance of Ca modified $(La_{1-x}Ca_x)_{9.67}(SiO_4)_6O_{2+\delta}$ ( $x = 0.0, 0.05, 0.10$ and $0.15$ )	155
Fig.5.3	SEM micrographs and grain histograms of Ca modified $(La_{1-x}Ca_x)_{9.67}(SiO_4)_6O_{2+\delta}$ ( $x =$	156

	0.0, 0.05, 0.10 and 0.15)	
Fig.5.4	Deconvoluted X-ray photoelectron spectroscopy measurements of Ca modified $(La_{1-x}Ca_x)_{9.67}(SiO_4)_6O_{2+\delta}$ ( $x = 0.0, 0.05, 0.10$ and $0.15$ )	157
Fig.5.5	(a) Grain size obtained from SEM micrographs (grain histograms) (b) La content extracted from XPS (c) Si content from XPS (d) O content from XPS (lines are a glide to eye)	159
Fig.5.6	Thermogravimetric curves for Ca modified $(La_{1-x}Ca_x)_{9.67}(SiO_4)_6O_{2+\delta}$ ( $x = 0.0, 0.05, 0.10$ and $0.15$ ) showing the variation of mass loss and $dm/dT$ with temperature	160
Fig.5.7	Arrhenius and NNH fitting of $\sigma dc$ -T curves for $x = 0, 0.05, 0.1$ and $0.15$ in $(La_{1-x}^{3+}Ca_x^{2+})_{9.67}(SiO_4)_6^{4-}O_{2+\delta}^{2-}$ system.	163
Fig.5.8	The universal exponent (p)-Temperature(T) plot for $x=0, x=0.1$ in $(La_{1-x}^{3+}Ca_x^{2+})_{9.67}(SiO_4)_6^{4-}O_{2+\delta}^{2-}$ system	164
Fig.5.9	Two-dimensional contour plot of $s$ versus $T$ and $\omega$ for $x = 0, x = 0.1$ in $(La_{1-x}^{3+}Ca_x^{2+})_{9.67}(SiO_4)_6^{4-}O_{2+\delta}^{2-}$ system	168
Fig.5.10	Overlapping Large Polaron Tunnelling (OLPT) fitting of parameter $s$ -T curves at $\omega = 10^3, 10^4, 10^5$ and $10^6$ ( $s^{-1}$ ) for $(La_{1-x}^{3+}Ca_x^{2+})_{9.67}(SiO_4)_6^{4-}O_{2+\delta}^{2-}$ system	169
Fig.5.11	a) Tunnelling distance with frequency and b) hopping energy with tunnelling distance at $\omega = 10^3, 10^5$ and $10^6$ ( $s^{-1}$ ). For $x = 0$ (square), $x = 0.1$ (circle) in $(La_{1-x}^{3+}Ca_x^{2+})_{9.67}(SiO_4)_6^{4-}O_{2+\delta}^{2-}$ system (lines are glide to eye)	170
Fig 5.12	(a) Variation of normalized optical (large polaron's) absorption for $x=0.0$ and $x=0.1$ in $(La_{1-x}^{3+}Ca_x^{2+})_{9.67}(SiO_4)_6^{4-}O_{2+\delta}^{2-}$ system(Inset) Valence band spectra using XPS study for both the samples along with zoomed valence band spectra in the negative binding	172

region (b) Tauc plots for direct band gap is estimated 4.2 eV and 4.05 eV respectively suggested wider exciton energy for  $x = 0.1$  (c) Free carrier absorption (FCA) fitting of the absorption obtained from UV-visible measurement for acoustic and optical phonon contributions (d) Ratio of phononic scattering coefficient ( $i =$  acoustic and optical phonon contributions) for  $x = 0.1$  and  $x = 0.0$ .

Fig. 5.13 Field dependent conductivity for  $x=0.0$  and  $0.1$  in  $(La_{1-x}^{3+}Ca_x^{2+})_{9.67}(SiO_4)_6^{4-}O_{2+\delta}^{2-}$  system, inset shows the ratio of conductivity for  $x=0.1$  and  $x=0.0$  173

Fig. 5.14 (a) Classical model for bound and unbound continuum states of large polaron self-trapped carrier. (b) Illustration of difference in electronic band structure for  $x=0.0$  and  $x=0.1$  in  $(La_{1-x}^{3+}Ca_x^{2+})_{9.67}(SiO_4)_6^{4-}O_{2+\delta}^{2-}$  system and polaronic states. (c) unit cell structure in the x-y plane in this c-axis is into plane at corner occupied by O4 and surrounded by La1(6h) site as mentioned earlier. (d)  $2 \times 2 \times 1$  supercell the long channel formation in ab-plane and increase in conductivity in apatite structure (O4-La1(6h) hexagon can be visualize in central gray oval) 175



---

## LIST OF TABLES

---

		Page No.
<b>Chapter I</b>	<b>Introduction and Literature Review</b>	
Table 1.1	Comparison between different fuel cells	6
<b>Chapter 2</b>	<b>Synthesis, Characterization and Analysis Techniques</b>	
Table 2.1	Specifications of the proposed materials	37
<b>Chapter 4</b>	<b>Influence of ionic radii on the conduction mechanism in Lanthanum silicate oxyapatite</b>	
Table 4.1	Wyckoff positions and occupancy obtained from refinement for Ba substituted samples	112
Table 4.2	Wyckoff positions and occupancy obtained from refinement for Ca substituted samples	113
Table 4.3	$\delta$ obtained from TGA and XPS in Ca substituted sample	121
Table 4.4	$\delta$ obtained from TGA and XPS in Ba substituted sample	122
<b>Chapter 5</b>	<b>Overlapping large polaron tunnelling in lanthanum silicate oxyapatite</b>	
Table 5.1	$\delta$ obtained from TGA and XPS	152



---

## PREFACE

---

The need for energy is increasing daily as a result of urbanization and industrialization, whereas conventional fossil resources like oil, coal, natural gas, etc., are quickly running out. These fossil fuels currently serve as our main source of fuel for meeting our energy requirements. However, there is serious cause for concern over the supply of fossil fuels in the coming years. The use of conventional energy sources is hampered by the burning of fossil fuels releasing harmful gases posing number of environmental risks. Global warming is possible by these negative environmental repercussions. The growing awareness of the energy crisis and greenhouse gas emissions has prompted a search for alternative routes. To identify an alternate potential for alternative pathways, the research is divided into two parts, first of which is focused on renewable and ecofriendly sources and second on electrochemical devices such as fuel cells.

Electrochemical devices for energy storage will play a crucial role in a world dependent on energy to address the fast depletion of fossil resources. Electrochemical devices either produce electricity from a chemical reaction (such as a battery) or use electrical energy to initiate a chemical reaction (like a catalyst). Among the many available electrochemical devices, fuel cells are the most efficient and offer a variety of advantages for mobile and stationary power generation, such as large-scale centralized power generation as well as power generation in individual homes and enterprises, etc.

There are currently a variety of fuel cell types available for purchase. Electrolyte substance is typically used to classify fuel cells. Their power outputs, operating temperatures, electrical efficiency, and common applications differ. Solid oxide fuel cells (SOFCs) are one of the cleanest and most efficient methods for directly converting a range of fuels to electricity. SOFCs powered by natural gas are ideally suited for distributed power generation, for instance. However, the commercialization of SOFC technologies is contingent on the development of new materials that can both cut costs and improve performance and durability.

One of the crucial hurdles to achieve high- performance SOFC systems is the electrolyte. Electrolyte sandwiched between anode and cathode is the central component of SOFCs which play a crucial role in the current conduction. In the cell, oxygen molecule has been converted into oxygen ions that must migrate through the electrolyte to the fuel side. It is a key component of SOFCs. For the migration of oxygen ions, electrolyte must possess a high ionic conductivity and no electrical conductivity. It must be fully dense to prevent short-circuiting of reacting gases throughout it. It should be thin also to minimize resistive loss in the cell. As with the other materials, it must be chemically, thermally, and structurally stable over a wide range of temperature.

Due to its pure ion conducting properties over a large range of oxygen partial pressures and ease of manufacture of high-density ceramics, yttria stabilized zirconia (YSZ) is widely employed as the solid electrolyte in most SOFCs. Apart from YSZ, there are other types of oxide ion conducting materials, including fluorite (doped  $\text{CeO}_2$  and  $\text{Bi}_2\text{O}_3$ ), Perovskite ( $\text{LaGaO}_3$ ,

LaAlO<sub>3</sub>), Brownmillerite (Ba<sub>2</sub>Ln<sub>2</sub>O<sub>3</sub>), Aurivillius (BIMEVOX), Pyrochlore (Gd<sub>2</sub>Zr<sub>2</sub>O<sub>7</sub>), LAMOX and Apatite-type oxide. Researchers are intrigued by the high oxide ionic conductivity of apatite-type lanthanum silicate oxide materials, which is equivalent to typical oxide ion conductors such as yttria stabilized zirconia. With the general formula  $La_{9.33+x}Si_6O_{26+1.5x}$  ( $x = 0-0.67$ ), lanthanum silicate apatite (LSA) exhibits a high conductivity in the intermediate temperature range and a high oxygen transference number over a broad range of oxygen partial pressures. The apatite-type phases  $La_{10}Si_6O_{27}$  have generated a lot of interest as possible electrolytes for solid oxide fuel cells (SOFCs). Low activation energy for ionic conduction and relative stability characterizes apatite. Rare earth cations are present in the apatite crystal's seventh and ninth coordinated cavities. Apatite-type lanthanum silicates are composed of lone tetrahedral SiO<sub>4</sub> units, which have a space group P6<sub>3</sub>/m in their hexagonal crystal structure. The remaining oxygen ions are dispersed via one-dimensional channels throughout the structure. Strong conduction has been seen as a result of a process in which interstitial oxygen ions migrate through cavities positioned along the c-axis between La channels and isolated SiO<sub>4</sub> tetrahedra. According to neutron powder diffraction atomistic computer modeling and HRTEM observation, which differ from other oxide-ion conductors, the oxygen ion journey in LSA happens by an interstitial-type transport mechanism. The conductivity of LSO rises with La concentration in  $La_{9.33+x}Si_6O_{26+1.5x}$  because additional oxygen ions are injected into the interstitial location of the lattice. Below 650°C,  $La_{9.92}Si_6O_{26.88}$  gives a better conductivity than YSZ. As a result, numerous researchers have explored the all-possible mechanism of conduction in apatite bases ion conductors

The apatite based FOICs (discovered by Nakayama in 1995) showed high ionic conductivity like perovskite based FOICs in low temperature regime (LTR). Among these FOICs, due to its anisotropic ion conduction ( $\sigma_c^{\parallel}/\sigma_c^{\perp} > 10$ ), lanthanum silicate oxyapatite i.e.,  $La_{10-\alpha}^{3+}(SiO_4)_6^{4-}O_{2+\delta}^-$  (LSO) is most interesting and attracted the researcher. Various experiments and theoretical studies predict that  $O_{int}$  (interstitial Oxygen) promotes cooperative movements between the O4 ion and excess oxygen is introduced as interstitial charge carriers to maintain electrical neutrality with La ions. There are 4 channels proposed for the conduction. Channels no. 1 and 2 are formed by the oxygen vacancies in between La(4f)-O4, channel no. 3 is nearest to the Si vacancy site and channel no. 4 is linked to the formation of oxygen Frenkel defects. Thus, there is scope of conductivity enhancement in polycrystalline LSO. In polycrystalline sample, grain alignment and doping are the two common methods to get the desired properties in the sample, the same has been employed by various research groups in the last few years. Grain alignment and c-axis alignment is done by various methods such as sol-gel and arc melting, respectively. Various doping such as Al, Mg at B-site and Alkaline earth and rare earth substitutions at A-site have been done in order to get conductivities in the range of 1 S/cm but unfortunately, conductivity is achieved in the range of 10-50 mS/cm. Though the two kind of conduction mechanism, namely, push pull and interstitial are well described for the oxyapatite but its dynamics is still scarce at large. Thus, in the present thesis, we are investigating the alteration in the structural and dynamics disorder with various substitution in the LSO.

In order to understand the conductivity of LSO and its composition as an

electrolyte material we synthesized the lanthanum silicate  $\text{La}_{9.67}\text{Si}_6\text{O}_{26.5}$

The present thesis is divided into seven chapters and a brief description is given below:

**Chapter 1** It begins with a brief introduction to fuel cells and continues with an exhaustive review of the relevant literature. This chapter discusses the background and fundamentals of fuel cells, the essential requirements of fuel cell components, the mechanism and kinetics for the components of the SOFC, the materials selection for electrolyte, and the conduction mechanism of the apatite-based electrolyte materials. It also explains the motivation behind the research work that was done. This chapter contains the primary purpose of the study that is being presented here as well.

**Chapter 2** discusses various experimental techniques used for the present investigations. It represents the details of implemented experimental instruments, analysis techniques and solid-state synthesis route adopted to synthesize the samples. A detailed description of employed instruments such as TGA, DSC, XRD, SEM, XPS, and impedance measurements, etc. along with the important analysis techniques like Rietveld Refinement analysis has also been discussed in this section. We also discussed the migration analysis using softBV application.

**Chapter 3** The apatite type single phase  $\text{La}_{9.67}\text{Si}_6\text{O}_{26.5}$  samples was synthesized by solid state reaction route method. XRD patterns confirms the formation of pure crystalline apatite-type single phase with hexagonal structure having space group  $P6_3/m$ . Rietveld refinement of the XRD data reveals the crystallographic

information of the system. Thermal study shows the formation of well crystallized lanthanum silicate apatite sample. SEM characterization reveals that particles are highly dense but agglomerated and average grain size was found 2-5  $\mu\text{m}$ . Conductivity spectroscopic technique shows that conduction is due to mainly mobile oxide ions. Dimensionality has been calculated based on Jonscher's power law exponent factor and it was found the predominantly one-dimensional migration of oxide ion through the interstitials. This was further confirmed by the bond balance energy landscape analysis of the system. Sample (sintered at high temperature of 1400  $^{\circ}\text{C}$ ) shows low activation energy ( $E_a = 0.69$  eV) with the very high dc conductivity of about  $1.4 \times 10^{-2} \text{ Sm}^{-1}$ , measured at 700  $^{\circ}\text{C}$ . This indicates that this system can be used as solid electrolyte for SOFC applications.

In **Chapter 4, We** discussed the influence of the ionic radii on the conduction mechanism in lanthanum silicate oxyapatite, with the alteration of La site with different ionic radii to form  $(\text{La}_{1-x}\text{A}_x)_{9.67}(\text{Si O}_4)_6\text{O}_{2+\delta}$  ( $x = 0.0, 0.05, 0.10, 0.15$ ) where  $\text{A} = \text{Ca}$  and  $\text{Ba}$ . The ionic radii of substituents will alter the average area of critical triangle (saddle point). The structural, microstructural, electronic and conductivity studies was performed using XRD, SEM, XPS and impedance measurement. With ionic radii variation, ion mobility volume has risen to nearly 3 times in Ca substituted sample than Ba substituted sample. We have obtained La deficient Ca substituted samples and O deficient Ba substituted samples. Further, XPS, TGA and Rietveld refinement confirm the formation of La and O deficient Ca and Ba substituted samples, respectively.

In **Chapter 5**, A series of apatite-based lanthanum silicate  $(La_{1-x}A_x)_{9.67}(SiO_4)_6O_{2+\delta}$  ( $x = 0.0, 0.05, 0.10, 0.15$ ) with Ca doped was synthesized using the high temperature solid-state route and their conductivity probed. Powder X-ray diffraction was used to determine the phase formation and structure of the prepared oxides. SEM analyses confirm the morphology of prepared catalysts. This series of apatite-based oxide materials exhibit higher oxide ion conductivity with lower activation energy and the activation energy increases with La vacancies. We have obtained La deficient and O rich samples with Ca substitution. The conductivity, due to connected grain growth increased for  $x = 0.1$ .

**Chapter 6** concludes the outcomes of the research works of this thesis and propose the future scope of the present investigations.

